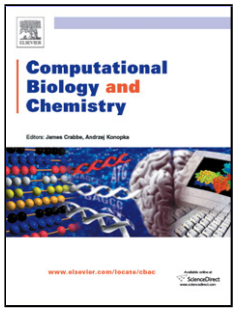

Title: Zooming-in on cancer metabolic rewiring with tissue specific constraint-based models

Author: Marzia Di Filippo Riccardo Colombo Chiara Damiani Dario Pescini Daniela Gaglio Marco Vanoni Lilia Alberghina Giancarlo Mauri

PII: S1476-9271(15)30014-1
DOI: http://dx.doi.org/doi:10.1016/j.compbiolchem.2016.03.002
Reference: CBAC 6528

To appear in: *Computational Biology and Chemistry*

Received date: 27-5-2015
Revised date: 25-2-2016
Accepted date: 4-3-2016

Please cite this article as: Marzia Di Filippo, Riccardo Colombo, Chiara Damiani, Dario Pescini, Daniela Gaglio, Marco Vanoni, Lilia Alberghina, Giancarlo Mauri, Zooming-in on cancer metabolic rewiring with tissue specific constraint-based models, *<![CDATA[Computational Biology and Chemistry]]>* (2016), http://dx.doi.org/10.1016/j.compbiolchem.2016.03.002

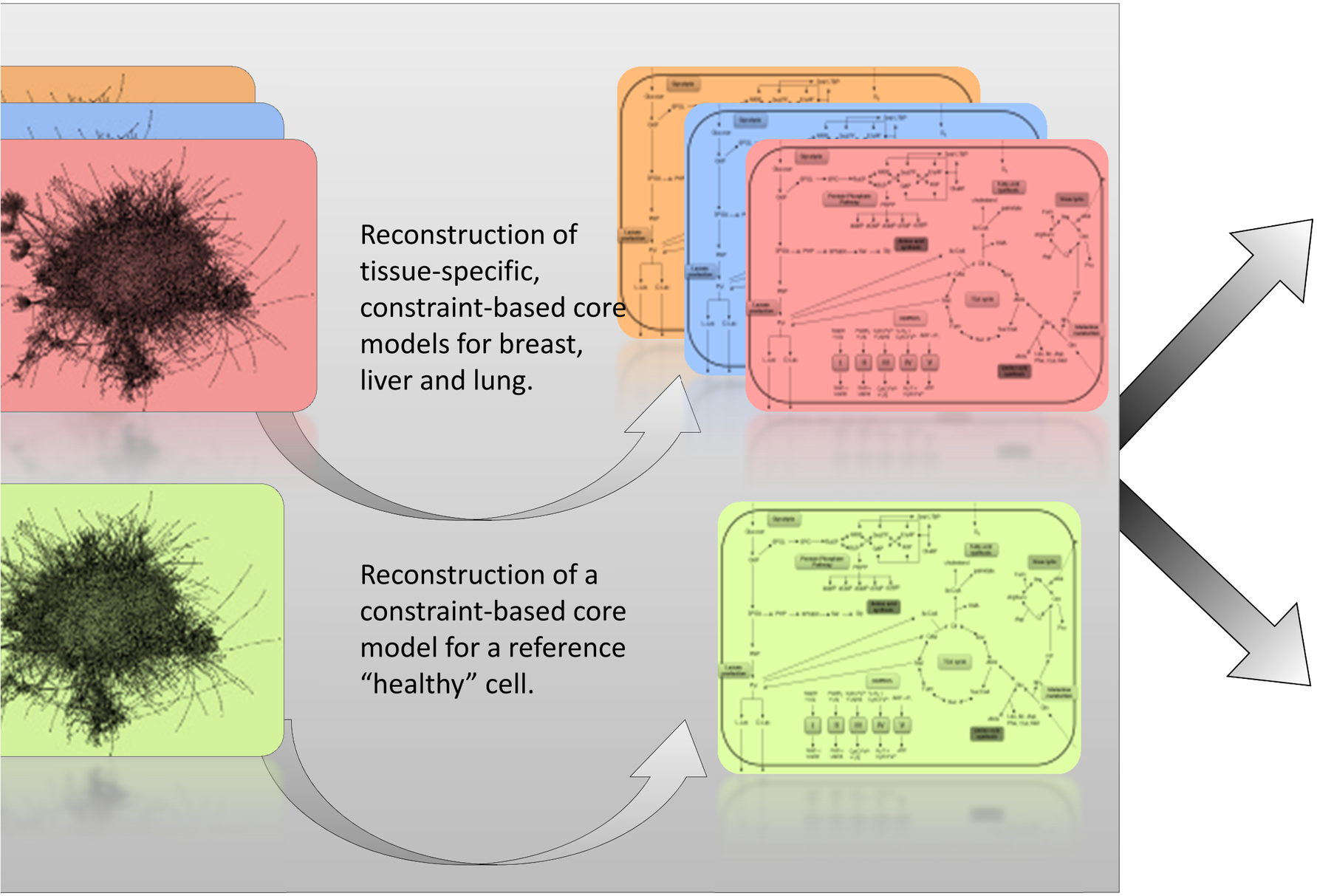

A)

DHAP[c] <=> GAP[c]

GAP[c] + NAD[c] + Pi[c] -> 1,3-bisphospho-D-glycerate[c] + H[c] + NADH[c]

1,3-bisphospho-D-glycerate[c] + ADP[c] -> 3-phospho-D-glycerate[c] + ATP[c]

3-phospho-D-glycerate[c] -> 2-phospho-D-glycerate[c]

2-phospho-D-glycerate[c] -> H2O[c] + PEP[c]

ADP[c] + PEP[c] -> ATP[c] + pyruvate[c]

B)

H2O[c] <=> H2O[m]

AKG[c] <=>

isocitrate[m] + NAD[m] -> AKG[m] + CO2[m] + H[m] + NADH[m]

isocitrate[m] + NADP[m] -> AKG[m] + CO2[m] + H[m] + NADPH[m]

GTP[c] + OAA[c] -> PEP[c] + GDP[c] + CO2[c]

A) Reversion of the tumoral phenotype.
B) Identification of fragility points.

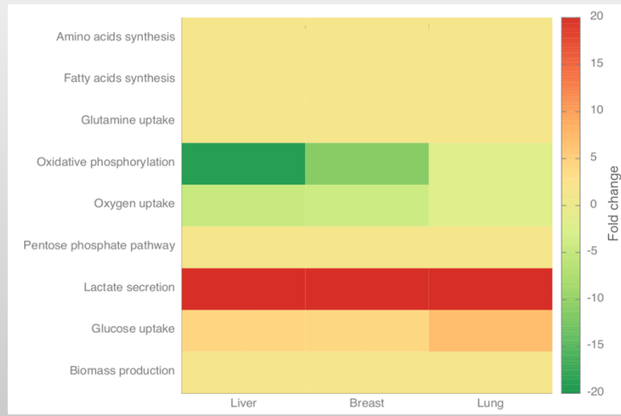

Up- and down-regulations within metabolic pathways considered in this an

Highlights

- In the context of metabolic networks, genome-scale modeling represents an increasingly used approach, as it has been shown to be successful in modeling the entire human, as well as cancer cells metabolism for the prediction of selective drug. In spite of the potentialities linked to their comprehensiveness, these reconstructions are difficult to control and often include errors, such as improper filling of network gaps.

- Starting from already existing genome-scale metabolic models, we aim at reconstructing manually curated core models that zoom-in on cancer metabolic rewiring. In order to study the role of the Warburg effect and more in general the role of all cancer metabolic alterations in supporting the neoplastic proliferation, we focused on the three most harmful neoplasias: liver, breast and lung tumors.

- Even though some metabolic features are associated with most cancer cells, several variations may emerge in specific tumor types. Following the reconstruction of the core metabolic models, we estimated the optimal flux distribution for each of them with FBA.

- We carried out two different analyses on the reconstructed core models. The aim of the first one is to highlight the reactions responsible for a reversion of the tumoral phenotype toward the reference model, whereas the second one has as purpose the identification of all the possible fragility points in the cancer models, which are able to cause, if inhibited, a negative effect on the system.

- We observed a clear distinction between reference and cancer condition under several aspects: growth rate, emergence of the Warburg effect, lactate secretion, glucose and glutamine uptake, TCA cycle, and the oxidative phosphorylation flux values.

- We also observed heterogeneity in terms of flux values not only between reference and cancer conditions, but also among the three different cancers, concerning some key pathways, which are glycolysis, TCA cycle and OXPHOS.

- Results strengthens the need to focus the attention on several types of tumors rather than on a generic cancer cell, because, although some metabolic features are associated to the three cancers, relevant variations emerged among them.

Zooming-in on cancer metabolic rewiring with tissue specific constraint-based models

Marzia Di Filippo[1,2]; Riccardo Colombo[1,2]; Chiara Damiani[1,2]; Dario Pescini[1,3,*]; Daniela Gaglio[1,5]; Marco Vanoni[1,4]; Lilia Alberghina[1,4]; Giancarlo Mauri[1,2].

[1] *SYSBIO Centre of Systems Biology, Piazza della Scienza 2, 20126 Milano, Italy*
[2] *Dipartimento di Informatica, Sistemistica e Comunicazione, Università degli Studi di Milano-Bicocca, Viale Sarca 336, 20126 Milano, Italy*
[3] *Dipartimento di Statistica e Metodi Quantitativi, Università degli Studi di Milano-Bicocca, Via Bicocca degli Arcimboldi 8, 20126 Milano, Italy*
[4] *Dipartimento di Biotecnologie e Bioscienze, Università degli Studi di Milano-Bicocca, Piazza della Scienza 2, 20126 Milano, Italy*
[5] *Istituto di Bioimmagini e Fisiologia Molecolare, Consiglio Nazionale delle Ricerche, Via F.lli Cervi 93, 20090 Segrate (MI), Italy*

Abstract

The metabolic rearrangements occurring in cancer cells can be effectively investigated with a Systems Biology approach supported by metabolic network modeling. We here present tissue-specific constraint-based core models for three different types of tumors (liver, breast and lung) that serve this purpose. The core models were extracted and manually curated from the corresponding genome-scale metabolic models in the Human Metabolic Atlas database with a focus on the pathways that are known to play a key role in cancer growth and proliferation. Along similar lines, we also reconstructed a core model from the original general human metabolic network to be used as a reference model.

A comparative Flux Balance Analysis between the reference and the cancer models highlighted both a clear distinction between the two conditions and a heterogeneity within the three different cancer types in terms of metabolic flux distribution. These results emphasize the need for modeling approaches able to keep up with this tumoral heterogeneity in order to identify more suitable drug targets and develop effective treatments. According to this perspective, we identified key points able to reverse the tumoral phenotype towards the reference one or vice-versa.

Keywords: Cancer metabolic rewiring; Network reconstruction; Core metabolic model; Flux Balance Analysis.

1. Introduction

Over the past decades, a large quantity of information has been gathered about the main metabolic differences between cancerous cells and their healthy counterparts [1]. Fundamental differences in the metabolism of normal cells and rapidly proliferating cancer cells were already observed in 1924, when Otto Warburg detected a reprogramming of glucose metabolism in tumor cells also known as "Warburg effect" [2, 3]. According to this phenomenon, cancer cells metabolize large quantities of glucose into lactate by a fermentative metabolism regardless of oxygen availability, as opposed to normal cells, which mainly rely on mitochondrial oxidative phosphorylation to generate the energy required for cellular processes. More recently, it has been suggested that a global *cancer metabolic rewiring* is performed in order to more effectively support the neoplastic proliferation replacing the metabolic program that operates in normal cells, which involves also a stimulated utilization of glutamine by reductive carboxylation [4] and an alteration of redox processes [5].

Given the complexity and nonlinearity of metabolism, a focus narrowed on the single molecules or mechanisms responsible for carcinogenesis fails to capture the complexity of cancer metabolic rewiring. Attention on the complex network of interactions in which they are involved, typical of Systems Biology [6, 7, 8, 9], is therefore required for the purpose. In this regard, mathematical models, which are formal and simplified representation of real systems, help to handle this complexity, maintaining at the same time a high level of accuracy and detail [10].

In particular, in the context of metabolic networks, genome-scale modeling represents an increasingly used approach [11], as it has been shown to be successful in modeling the entire human metabolism [12, 13, 14, 15], as well as cancer cells metabolism for the prediction of selective drug targets [16, 17, 18, 19]. In spite of the potentialities linked to their comprehensiveness, these reconstructions are difficult to control and often include errors, such as improper filling of network gaps (i.e. missing metabolic reactions

*Corresponding author; dario.pescini@unimib.it

that prevent the production or consumption of one or more metabolites). Moreover, the interpretation of the outcomes of their simulation is not always straightforward due to the difficulty in rationalizing such amount of data. On the other hand, *core models*, which limit the scope to specific aspects of metabolism, require more assumptions and a higher level of abstraction; nevertheless, they can be more accurately curated, their underlying assumptions are explicit, they are simpler, and thus their analysis might be more effective in uncovering system-level properties of cancer metabolic rewiring.

In view of this, starting from already existing genome-scale metabolic models, we aim at reconstructing manually curated core models that zoom-in on cancer metabolic rewiring. In order to study the role of the Warburg effect and more in general the role of all cancer metabolic alterations in supporting the neoplastic proliferation, we did not model a generic cancer cell, but rather we focused on the three most harmful neoplasias, in terms of incidence, mortality and prevalence, according to the last estimations in GLOBOCAN [20, 21]: liver, breast and lung tumors.

In fact, even though some metabolic features are associated with most cancer cells, several variations may emerge in specific tumor types [19, 22]. Cancer specific models may therefore be useful in identifying specific drug targets, paving the way towards a more personalized medicine.

2. Materials and methods

2.1. Flux Balance Analysis

Flux Balance Analysis (FBA) [23, 24, 25, 26] is a constraint-based method that allows to quickly calculate the flux of metabolites (i.e., the rate at which every metabolite is consumed or produced by each reaction) through all the reactions of a metabolic network, without requiring any information about kinetic parameters or metabolite concentrations. FBA assumes that the time variation of internal metabolite concentrations is equal to zero (pseudo-steady state assumption) and proceeds with an iterative application of constraints (reaction thermodynamics and capacity constraints) on the evaluated system [26] in order to exclude flux distributions from the space of allowable ones [27].
Assuming than that the cell behavior is optimal with respect to a certain objective, FBA exploits linear programming to identify an optimal flux distribution within the defined

solution space according to an objective function (as e.g. production of biomass or ATP yield) [26].

2.2. Human Metabolic Atlas

To investigate the metabolic processes of specific human cancer types, we exploited the Human Metabolic Atlas (HMA), a database which contains genome-scale metabolic networks for 69 cell types and 16 cancer types in addition to a generic and aspecific human metabolic model: the Human Metabolic Reaction (HMR) database, which has been constructed by merging elements of previously published generic genome-scale human metabolic models (Recon 1 [12], EHMN [13]) and by incorporating information from different databases such as HumanCyc [28] and KEGG [29, 30]

The specific models represent portions of the generic HMR that are expressed (or "active") in each tissue or cell type, according to biological evidence. In particular, cell type specific proteomic data contained in the Human Proteome Atlas (HPA) database [31] and tissue specific gene expression data and metabolomic data from the Human Metabolome Database (HMDB) [32, 33, 34] were integrated by applying the INIT (Integrative Network Inference for Tissues) algorithm [17]. Based on these different kinds of "omics" data, INIT assigns weights to the reactions in the HMR according to their different levels of evidence in the specific tissue or cell type. An optimization process is then performed with the aim of maximizing as much as possible the reactions fluxes with a high weight (since the corresponding enzymes have a high expression level) while minimizing the others. Reactions that carry flux in the obtained optimal flux distribution are assigned to the tissue or cell specific model.

2.3. Metabolic network reconstruction process

Starting with the genome-scale networks, we manually reconstructed constraint-based core metabolic models for the three different types of cancers and for a generic aspecific reference cell, by extracting those metabolic pathways having a relevant role in supporting cancer cells growth and proliferation [5, 35].

The reconstruction process of these models was not limited to the selection of the reactions of interest, but also involved the integration of all the elements required to perform FBA, such as transport and exchange reactions.

The former are essential to allow metabolites transport between compartments, while the latter define the enviromental constraints and may be subdivided into sinks (defining the cell nutrients) and demands (defining compounds secreted by the cell). Exchange reactions were also used to represent non modeled metabolites pertaining to pathways not included here.

As a final step, we performed an accurate manual curation of the developed core models in order to check the presence of incorrect reactions, as well as network gaps. This curation phase strongly relied on the biological database KEGG and on the most up-to-date human metabolic reconstruction Recon 2[15].

2.4. Topological analysis of the reconstructed metabolic models

A topological analysis has been performed on the reconstructed core models with the aim of examining their structural properties, by using the software Cytoscape [36, 37], and more precisely its plugin NetworkAnalyzer. In order to characterize the topology of the metabolic networks, we calculated the node degree distribution and the clustering coefficient for every metabolic network. We refer the reader to the review in [38] for an exaustive description of the above mentioned metrics.

2.5. Differential analysis of flux distributions

Following the reconstruction of the core metabolic models, we estimated the optimal flux distribution for each of them with FBA. In order to compare the capabilities of cancer cells with respect to normal cells to cope with the same metabolic requirements, given an identical medium composition, we did not impose specific flux values for nutrient uptakes, but we imposed the same arbitrary value (1000), while we left the flux in the allowed direction unbounded for all internal reactions. For the same reason, although specific biomass formation pseudo-reactions representing the conversion of biomass precursors into biomass are provided in the original genome-wide models, we used the same formulation as objective function for both types of cells.

The simulations have been performed using the COBRA (COnstraint Based Reconstruction and Analysis) Toolbox [39, 40] and the GLPK linear programming solver. Each

obtained flux distribution has been evaluated to check the absence of possible thermodinamically infeasible loops by using the algorithm developed in [41].

Once that flux distributions free from thermodynamical infeasible loops were obtained, we compared each cancer model with respect to the reference model, computing the fold change for each reaction as the ratio of the corresponding flux value in the cancer model versus its flux value in the reference one. It is worth stressing that the choice of using the same reference model, rather than comparing each tumor against its corresponding healthy model, is essential in order to make the three cancer models comparable among themselves and making the differential analysis meaningful.

2.6. Identification of critical reactions

We carried out two different analyses on the reconstructed core models. The aim of the first one is to highlight the reactions responsible for a reversion of the tumoral phenotype toward the reference model, whereas the second one has as purpose the identification of all the possible fragility points in the cancer models, which are able to cause, if inhibited, a negative effect on the system.

Identification of reactions responsible for the phenotype reversion. This analysis aims to identify the structural differences in the core metabolic networks that are mainly responsible for their dissimilarities in terms of flux distributions.

In attempting to reach this goal, it is necessary to identify the reactions that are differentially present in the four core models.

We determined the set of reactions that are present only in the reference model and we added them in a stepwise fashion to the cancer models in order to investigate the effect of each perturbation. We also identified the reactions shared by all tumor models, but not present in the reference one. Such reactions were included in the reference model to evaluate whether a flux distribution typical of cancer cell could be obtained. Along similar lines, we removed these reactions from the tumor models to assess if their removal caused a reversion of the tumoral phenotype towards the reference one.

Identification of cancer networks fragility points. In order to identify fragility points in the reconstructed cancer models, we examined the "extent" of the Warburg effect in each of them through the quantification of two indexes, as proposed in [42]:

- the glycolytic to oxidative ATP flux ratio (AFR)
- the ratio of the glycolytic versus oxidative capacity (EOR), computed as the fraction of extracellular acidification rate (i.e. lactate secretion flux value), over the oxygen consumption rate (i.e. oxygen consumption flux value).

Given that high AFR and EOR ratios denote tumors with a "high" Warburg level (as explained in [38]), we queried those reactions that, if inhibited, reduce the Warburg effect, by decreasing the AFR and EOR ratios. The simulation of each metabolic reaction inhibition (and then, of the corresponding enzyme) has been performed by constraining the flux through each reaction to zero.

We also searched for those reactions that, after inhibition of the corresponding enzyme, lead to a reduction of the biomass synthesis rate. It has indeed been suggested that the above mentioned indexes are positively associated to cancer cell migration, but may have no effect on cell proliferation [42], in which we are interested.

3. Results and discussion

3.1. Core metabolic tissue-specific cancer models

The three reconstructed core metabolic tissue-specific cancer models consist of three cellular compartments (cytosol, mitochondria and external environment), and include those metabolic pathways having a relevant role in cancer cells growth [5, 35], namely glycolysis, pentose phosphate pathway (PPP), tricarboxylic acid cycle (TCA cycle), oxidative phosphorylation, glutamine metabolism, amino acid synthesis, urea cycle, folate metabolism and palmitate synthesis. Sink reactions for glucose, glutamine and oxygen have been added in the reconstructed core models for defining the medium composition. The modifications with respect to the original genome-wide models emerging from the curation process are listed in Table 1.

The detailed lists of the reactions included within each of the final core models are available in Supplementary materials (S1_HMR_CORE.xls, S2_LIVER_CANCER_CORE.xls, S3_BREAST_CANCER_CORE.xls, S4_LUNG_CANCER_CORE.xls). Table 2, instead, shows the number of metabolites and reactions of the core models, as compared to their genome-wide counterparts. Models are also accessible in the BioModels Database [43]

Original reactions	Revised reactions	Compartment
–	3-phospho-D-glycerate ⇒ 2-phospho-D-glycerate	Cytosol
Acetyl-CoA + H_2O + OAA ⇔ Citrate + CoA	Acetyl-CoA + H_2O + OAA ⇒ Citrate + CoA	Mitochondria
Isocitrate + NAD^+ ⇒ AKG + CO_2 + H^+ + NADH	Isocitrate + NAD^+ ⇔ AKG + CO_2 + H^+ + NADH	Mitochondria
Isocitrate + $NADP^+$ ⇒ AKG + CO_2 + H^+ + NADPH	Isocitrate + $NADP^+$ ⇔ AKG + CO_2 + H^+ + NADPH	Mitochondria
AKG + Leucine ⇒ 4-methyl-2-oxopentanoate + Glutamate	4-methyl-2-oxopentanoate + Glutamate ⇔ AKG + Leucine	Cytosol
AKG + Isoleucine ⇒ 2-oxo-3-methylvalerate + Glutamate	2-oxo-3-methylvalerate + Glutamate ⇔ AKG + Isoleucine	Cytosol

Table 1: Revised reactions after the curation phase of the core models, performed consulting KEGG database and the human metabolic reconstruction Recon 2. The first reaction is the result of a gap correction found within the glycolysis pathway, which in the starting genome-scale models, has been erroneously filled with two exchange reactions for the metabolites 3-phospho-D-glycerate and 2-phospho-D-glycerate. A revision of the directionality has been done for the other five reactions. In particular, the third and fourth reactions have been corrected within the cancer models because it is known that in tumors, unlike normal cells, the enzyme that is responsible for these reactions (isocitrate dehydrogenase) works mainly in the reverse direction.

with the identifiers MODEL1502100000, MODEL1502100001, MODEL1502100002 and MODEL1502100003.

From the topological analysis, as expected [38], it emerged that all the four models exhibit a hierarchical topology, that is a structural organization of the network integrating the scale-free property and the presence of modules. In the context of metabolic networks, modules usually overlap with metabolic pathways, while the scale-free topology is characterized by the presence of few species taking part in a high number of reactions, called hub (e.g. cofactors as ATP or NADH), and a huge number of metabolites taking part in a small number of reactions. Moreover, these models are marked by the presence of the ultra small-world property [38], a feature that is correlated to a fast transmission of the information through the network. As a consequence of this property, local perturbations in metabolites levels can quickly affect the entire network. At last, it has also emerged from the analyzed networks that the most part of the interactions are established between hub and species having few interactions. This property, called disassortativity, reflects the fact that elimination of a hub implies a strong negative effect on the entire network.

3.2. Tissue-specific cancer redistributions of metabolic flux

An overall understanding of the biological mechanisms behind cancer cells growth and proliferation requires a complete and accurate analysis of the metabolic flux redistribution

	Genome-scale		Core	
Model	# reactions	# metabolites	# reactions	# metabolites
HMR database	8180	6011	274	252
Liver Cancer GW	4386	4020	257	242
Breast Cancer GW	4299	3955	243	233
Lung Cancer GW	3809	3653	235	230

Table 2: Number of reactions and metabolites for each of the genome-scale and core metabolic models

that they undergo [44]. In this work, we exploited FBA to quantify the metabolic flux through reactions of reference and tumor cells and, above all, to emphasize both the up- and down-regulations emerging between cancer and reference models, as long as the considered metabolic pathways are concerned. As objective function, we maximized the biomass production pseudo-reaction that was equally associated to all cancer genome-scale models, which has been adapted to encompass only the subset of metabolites needed for biomass production that are involved in the pathways here considered, each of them characterized by a proper stoichiometric coefficient, as showed in Table 3.

Biomass production reaction
0.4202 Alanine[c] + 0.00328 AMP[c] + 2.4523 Aspartate[c] + 0.00328 Arginine[c] + 0.03272 CMP[c] + 0.00805 dAMP[c] + 0.00537 dCMP[c] + 0.00537 dGMP[c] + 0.00805 dTMP[c] + 0.67628 Glutamine[c] + 0.5942 Glutamate[c] + 0.49244 Glycine[c] + 0.03709 GMP[c] + 0.06369 Proline[c] + 0.13132 Serine[c] + 0.01963 UMP[c] + 0.00427 Cysteine[c] + 0.01313 Isoleucine[c] + 0.0394 Leucine[c] + 0.00657 Methionine[c] + 0.04268 Asparagine[c] + 0.01313 Phenylalanine[c] + 0.0197 Tyrosine[c] + 0.03755 Cholesterol[c] + 0.04 Palmitate[c] → Biomass[s]

Table 3: Biomass production reaction used as objective function. This reaction includes the metabolites needed for biomass synthesis that are involved in the pathways here considered, each of them characterized by a proper stoichiometric coefficient. "c" and "s" correspond, respectively, to cytosol and external environment compartments.

A visual representation of the resulting "active" network is provided in Figure 1 for the reference model, whereas the main outcomes of the differential analysis are summarized in Figure 2, in which red and green chromatic scales highlight, respectively, the detected up-regulations and down-regulations, in terms of flux value, for the cancer condition with respect to the reference one.

A clear distinction between the two studied conditions in terms of growth can be

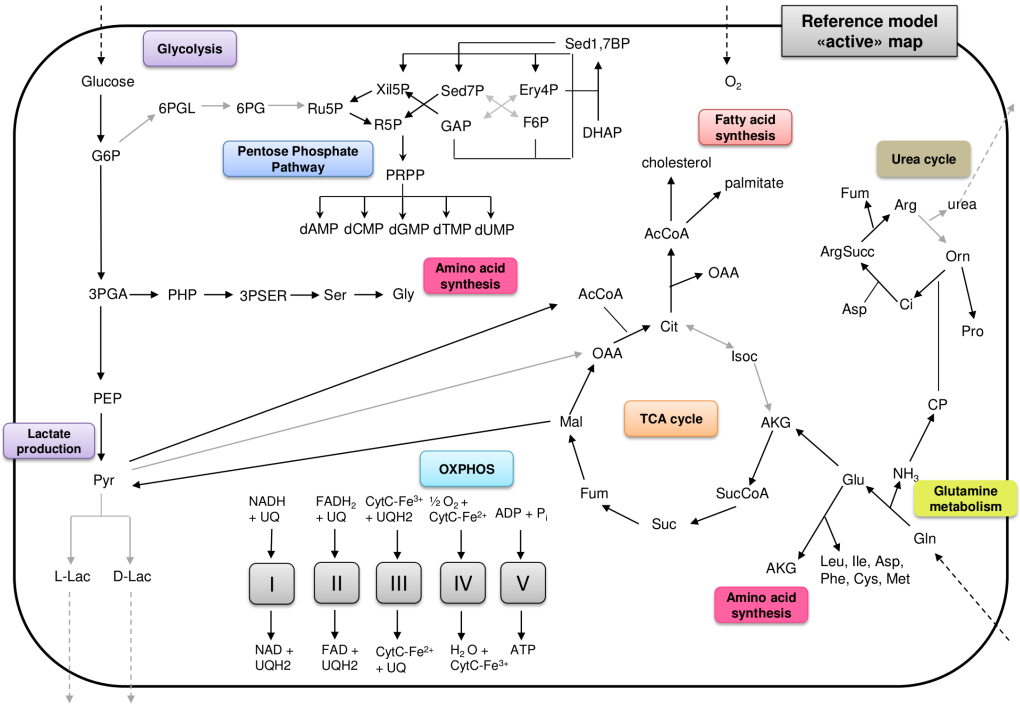

Figure 1: Schematic representation of the "active" network relative to the reference core model. This map shows, in a simplified view, the information concerning flux distribution in the reference core model within metabolic pathways under investigation in our work, namely glycolysis, pentose phosphate pathway, tricarboxylic acid cycle (TCA cycle), oxidative phosphorylation, glutamine metabolism, urea cycle, amino acid and fatty acid synthesis. The grey and black arrows correspond, respectively, to reactions having a null and a positive flux. The direction of each black arrow is set depending on the obtained flux value in the corresponding reaction. For reasons of space, cellular compartments are not included. Abbreviations: G6P, glucose-6-phosphate; 3PGA, 3-phospho-D-glycerate; PEP, phosphoenolpyruvate; Pyr, pyruvate; L-lac, L-lactate; D-lac, D-lactate; 6PGL, glucono-1,5-lactone-6-phosphate; 6PG, 6-phospho-D-gluconate; Ru5P, ribulose-5-phosphate; R5P, ribose-5-phosphate; Xil5p, xylulose-5-phosphate; GAP, glyceraldehyde 3-phosphate; Sed7P, sedoheptulose-7-phosphate; Sed1,7BP, sedoheptulose-1,7-bisphosphate; Ery4P, erythrose-4-phosphate; F6P, fructose-6-phosphate; DHAP, dihydroxyacetone phosphate; PRPP, phosphoribosyl pyrophosphate; UQ, ubiquinone; UQH2, ubiquinol; CytC-Fe2+, ferrocytochromeC; CytC-Fe3+, ferricytochromeC; Leu, leucine; Ile, isoleucine; Asp, aspartate; Phe, phenylalanine; Cys, cysteine; Met, methionine; Gln, glutamine; Glu, glutamate; Cit, citrate; Isoc, isocitrate; AKG, α-ketoglutarate; SucCoA, succinyl-CoA; Suc, succinate; Fum, fumarate; Mal, malate; OAA, oxaloacetate; AcCoA, acetyl-CoA; CP, carbamoyl-phosphate; Orn, ornithine; Pro, proline; Ci, citrulline; ArgSucc, argininosuccinate; Arg, arginine, PHP, 3-phosphonooxypyruvate; 3PSER, 3-phosphoserine; Ser, serine; Gly, glycine.

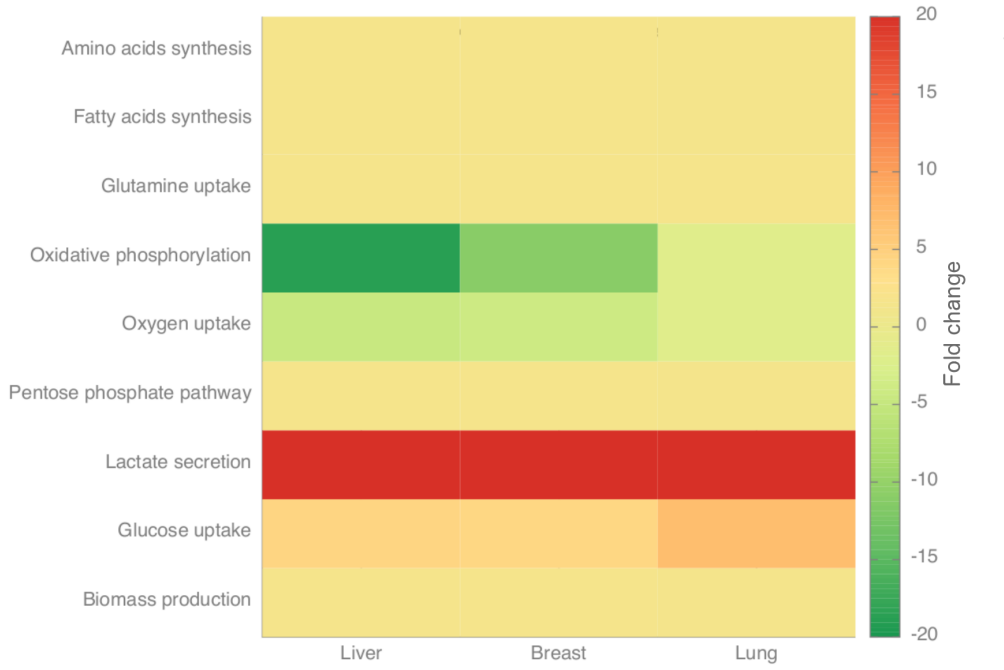

Figure 2: Main results obtained from the Flux Balance Analysis. Red and green chromatic scales correspond, respectively, to the detected up-regulations and down-regulations in the cancer cells models with respect to the reference model as result of fold change computation. From the figure it emerges that tumor cells, compared to the reference one, reprogram the metabolic pathways to satisfy their increased needs for the synthesis of macromolecular precursors essential for biomass production during tumor growth. Exploiting the FBA approach a heterogeneous behavior among the three investigated tumors also emerged.

observed. Indeed, the biomass production rate in cancer cells resulted higher than in reference ones, with a positive fold change of about 1.2-1.4 fold. This is an expected outcome considering that cancer cells are known to show abnormal proliferation and no contact inhibition [45]. It is meaningful to underline that, to support this higher proliferation rate, cancer cells must undergo a complete metabolic rewiring which affects all the pathways having a key role in cancer growth (i.e. the pathways considered in our analysis).

Going more into detail of the emerged dissimilarities, we detected in all three tumor models the presence of the Warburg effect (Figure 3). When comparing tumoral against reference cells, the flux analysis highlighted a strong dependence of the tumor cells on glycolytic metabolism and a shift from generation of ATP through OXPHOS pathway to glycolysis, even under a normoxic condition. Since it is known that glycolysis is less efficient than OXPHOS, relatively to the number of ATP molecules generated per unit of glucose consumed [46], cancer cells are expected to be constrained to increase their glucose uptake. Our cancer models are in line with this observation, as shown by a 4-7 fold upregulation of glucose uptake.

A consequence of this phenomenon is that most of the pyruvate produced, instead of entering in the TCA cycle, is redirected to lactate which is then excreted to the extracellular environment. Lactate secretion in cancer cells corresponds to the most known way to regenerate NAD^+ from NADH, balancing in this way the elevated glycolysis rate and allowing it to persist. Moreover, lactate secretion may be able to confer another advantage to tumor cells, enhancing their invasiveness by disrupting normal tissue architecture, and promoting an acidic tumor microenvironment to evade tumor-attacking immune cells [3].

At last, the relevance of an up-regulated glycolysis seems to be also linked to the pivotal relevance of this pathway from a biosynthetic point of view. In fact, the high glucose carbon flux through this pathway allows to divert some glycolytic intermediates toward the synthesis of the amino acids serine and glycine, and the pentose phosphate pathway [47, 48]. Both resulted up-regulated, respectively, by about 1.4-1.8 and 1.2–1.4 fold, since they allow the biosynthesis of some precursors required to assemble new cells [45].

The TCA cycle is another crucial pathway in the tumoral condition. Indeed, it emerged that, in addition to the generation of reducing equivalents for the oxidative phosphorylation, the TCA cycle also acts as a "hub" for biomass precursors production [49]. Several of its intermediates are used to synthesize molecules such as lipids and proteins, and, for this reason, a continuous efflux of metabolic intermediates from this pathway, such as oxaloacetate, α-ketoglutarate and citrate, is needed. In particular, the reductive carboxylation way, exploited to produce this last metabolite, has assumed a great relevance inside our analysis. Once the citrate is transported from the mitochondria to the cytosol, its metabolism provides acetyl-CoA for the synthesis of fatty acids (simplified in our models with the palmitate synthesis) and cholesterol, both required for the generation of the lipidic membranes. This justifies the up-regulation observed for the lipogenic enzymes ATP citrate lyase and fatty acid synthase of about 1.2-1.4 fold. The differential analysis of the fluxes revealed that, in contrast to what happens in the reference model (in which, as shown in Figure 1, the generation of citrate starts from the glycolysis-derived pyruvate, following the canonical direction of the TCA cycle), in cancer cells the conversions of mitochondrial pyruvate to acetyl-CoA and of oxaloacetate to citrate do not take place (null flux) (Figure 4). This implies, as a consequence, that inside the TCA cycle the level of citrate compared to that of the α-ketoglutarate becomes very low and, probably, this is the reason why cancer cells consider more advantageous having a reverse TCA cycle as the major pathway of citrate formation. Indeed, in each of the three tumor core models, a glutamine-dependent reductive carboxylation reaction occurs, catalyzed by the mitochondrial enzyme isocitrate dehydrogenase (IDH) which, differently from the reference cells, works in the reverse direction converting the α-ketoglutarate to citrate [49].

Glutamine has a key role in cancer growth and proliferation [50]. This has been confirmed in cancer fluxes analysis by the higher glutamine uptake (about 1.4 fold). This metabolite, together with glucose, represents a carbon and energy source to support many cellular processes, like reductive carboxylation and several biosynthetic pathways. Indeed, glutamine serves to maintain the pools of non essential amino acids, to provide a source of carbons for fatty acids synthesis, to produce aspartate (which is a required precursor for the synthesis of both nucleotides and the amino acids asparagine and arginine)

and, lastly, providing a source of oxaloacetate, to replenish the TCA cycle intermediates (i.e. performing anaplerosis, a crucial feature for cell growth and proliferation since it confers the ability to use the TCA cycle as a provider of precursors for the biomass synthesis). Moreover, a high anaplerotic flux is a more specific indicator of cell growth compared to a high glycolytic flux, since the latter is also stimulated by hypoxia and other stresses independently of the need to synthesize the biomass precursors [47].

A last typical cancer trait highlighted by the flux distribution analysis is a down-regulated oxidative phosphorylation which, together with an increased glycolysis, represents another aspect of the Warburg effect (Figure 5) [2]. In particular, a reduced activity of all the components of the OXPHOS, with a complete inhibition of the complex I activity and a sharp drop in the fluxes associated to other complexes occurred. Worth of note, downregulation of oxidative phosphorylation in lung cancer models was not as substantial as in the other two types of tumors: liver and breast. Indeed, as recently demonstrated by Hooda et al. in [51], the mitochondrial respiration is crucial in lung cells cancer and it promotes their progression and development.

The fluxes distributions obtained for each core model are available in Supplementary materials, Table S5.

3.3. Critical reactions

Stuctural differences responsible for cancer metabolic rewiring. Our core models have been analyzed in order to identify critical reactions able to cause a strong flux variation with the consequent reversion of the model phenotype, constituting potential anti-cancer targets.

Let us first focus on the reactions that appear only in the reference model and are absent in the cancer models (listed in Supplementary material, Table S6).

When analyzing the effect of their addition, one by one, to cancer models, it emerged that four of them are able to cause a perturbation in all three tumor types. These reactions are: 1) inorganic phosphate transport between cytosol and mitochondria; 2) water transport between cytosol and mitochondria; 3) the mitochondrial irreversible conversion from isocitrate to α-ketoglutarate catalyzed by NAD-specific form of isocitrate dehydrogenase (IDH) enzyme; 4) the mitochondrial irreversible conversion from isocitrate to α-ketoglutarate catalyzed by NADP-specific form of IDH enzyme.

1) The inorganic phosphate transport is based on a H^+/P_i cotransport catalyzed by the SLC25A3 enzyme. Its addition to cancer models produced a reduction of glucose uptake (between about 1.3 and 1.6 fold) and lactate secretion (between about 1.5 and 3 fold), and an enhancement of the ATP production by OXPHOS pathway (about 1.2 fold). Instead, the biomass synthesis rate showed no variation of its value and, therefore, the addition of this reaction causes a reduction of the Warburg effect but has no effect on cancer cells proliferation. This same reaction, even when removed from the reference model, produces an increase of the Warburg effect but has no consequence on cell proliferation rate. We remark that the decoupling between Warburg effect and proliferation has already been suggested (see [42] for further reference).

2) The second critical reaction is the water transport, catalyzed by the AQP8 enzyme. Its inclusion in cancer models caused a lowering of glucose uptake (between about 1.1 and 1.3 fold) and lactate secretion (between about 2 and 7 fold), and an increase of the ATP production by OXPHOS pathway (between about 1.2 and 2.5 fold). As in the previous case, there has been no decrease in biomass production rate. Its removal from the reference model reflected what we observed with the inorganic phosphate transport reaction.

What has emerged so far highlights the importance of transport reactions, towards which the focus is not generally posed in constraint-based analyses. In principle, the lack of these reactions in the cancer models would suggest a null expression level of the corresponding protein but a search within the HPA database has shown that their expression level is registered as medium-low. Therefore, some reactions, such as these two transports, are not removed from the models for the expression level of the corresponding protein, but due to the fact that after the optimization process they have a null flux.

3) and 4) The addition of the irreversible conversion from isocitrate to α-ketoglutarate catalyzed by NAD- and NADP-specific forms of IDH enzyme, has produced in cancer models a decrease of glucose uptake flux with a reduction or no production of lactate, and an increase, more evident in breast and lung cancer than in liver tumor,

of ATP production by OXPHOS pathway. Also in this case the flux associated with biomass synthesis has not changed its value after the perturbation.

After that, we identified all the reactions included in the three tumor models or in some cases at least in two of them, but that are absent in the reference model (see Supplementary material, Table S6). When investigating the effect of their addition to the reference model, we noticed that the demand reaction for α-ketoglutarate causes a reversion from an active OXPHOS to a more glycolytic phenotype even if the lactate production does not occur. In addition, this exchange reaction also produces an increase in cell proliferation rate of about 1.4 fold. The reference model showed a more "cancerous" behavior even after the replacement of the two irreversible reactions catalyzed by isocitrate dehydrogenase enzyme, with their reversible form. Indeed, after this modification, we observed a higher glucose and glutamine uptake, respectively of about 4 and 1.5 fold, production of lactate, a sharp drop of the OXPHOS pathway rate and an increase of the cell proliferation rate of about 1.5 fold. Lastly, although to a lesser extent, also the conversion reaction from oxaloacetate to phosphoenolpyruvate catalyzed by PCK1 enzyme caused a slight flux variation in the reference model. Indeed, even if the glycolytic flux remains very low and there is no production of lactate, a reduction of the ATP production by OXPHOS pathway (about 1.3 fold) and a nearly null variation of the biomass synthesis rate occur.

In the light of the considerations made on all the identified reactions that singularly caused a great flux variation, we tried to join together their activities. In the reference model, we combined the removal of inorganic phosphate and water transport reactions with the addition of the α-ketoglutarate exchange reaction and of PCK1-catalyzed conversion reaction from oxaloacetate to phosphoenolpyruvate and the reversible form of IDH-catalyzed reactions. This combination produced a full reversion of the reference model towards a cancer phenotype (see Supplementary materials, Table S7). Indeed, we measured, with respect to the original reference model, an increase of glucose and glutamine uptake, respectively, of about 4 and 1.4 fold, a high production of lactate, a reduced activity of all the components of the OXPHOS pathway with a complete inhibition of the complex I activity associated with a sharp drop of the flux associated with the reaction catalyzed by ATP synthase enzyme (about 13 fold), and a biomass synthesis

rate 1.4 fold higher.

This same set of reactions is involved in the reversion of the cancer models towards a phenotype very similar to that of the reference model (see Supplementary materials, Table S7). In particular, in breast and lung tumor models, we combined the addition of inorganic phosphate and water transport reactions with the removal of the α-ketoglutarate exchange reaction, the addition of the irreversible form of IDH-catalyzed reactions and the removal (in breast cancer) or addition (in lung cancer) of the PCK1-catalyzed reaction. After these changes, we observed a decrease of both glucose and glutamine uptake, respectively, of about 4–5 fold and 1.3–1.4 fold, no production of lactate, a completely functioning OXPHOS pathway with an up-regulation of ATP synthase activity of more than 10 fold in breast cancer and of about 1.4 fold in lung cancer (in which the ATP synthase flux is already high in the initial model), but also of the other complexes, and a decrease in biomass production rate of about 1.1–1.4 fold. The liver cancer represents an exception due to the fact that this same set of changes produced different results as compared to lung and breast cancers: although the perturbation similarly results in an interruption of lactate production, the glucose uptake rate enhances by 1.5 fold, the OXPHOS pathway fluxes remain very low, and neither the glutamine uptake nor the biomass synthesis rate is modified. Therefore, we decided to focus our attention on other reactions that are present in the reference model but not in the liver cancer model. We observed that the addition of the L-glutamate 5-semialdehyde transport reaction between cytosol and mitochondria, together with the previous changes, causes a complete reversion of the liver cancer model. Indeed, a decrease of both glucose and glutamine uptake, respectively, of about 4 fold and 1.4 fold, no production of lactate, a completely functioning OXPHOS pathway with a deep up-regulation of ATP synthase activity and, at last, a decrease in biomass production rate of about 1.4 fold occur.

Remarkably, the heterogeneity of the responses of different cancer types to a given perturbation supports the importance of developing cancer type-specific models.

Fragility points of cancer networks. Since a high number of marked differences have emerged from the analysis of fluxes distribution in reference and cancer core models, it is interesting to identify which reactions are responsible for the flux rewiring between the two conditions under consideration. Given that we are studying cancer cells growth,

we decided to focus on all the metabolic reactions that, after an inhibition, are able to cause a reduction of the flux associated with the biomass synthesis, because they could potentially represent drug targets for cancer treatment. Therefore, we performed single "in silico" inhibitions for each reaction of the three cancer core models and we then assessed the effect of these perturbations on flux distribution within the model. Among the identified reactions, we considered those that imply a strong reduction of the biomass synthesis rate (by at least 40–50%), which are likely potential targets to counteract the tumor growth.

In every cancer core model, the highest reduction of biomass has been caused by reactions belonging to the glycolytic pathway (see Supplementary materials, Table S8). Here, we observed that, after the inhibition of the glycolytic enzymes, cancer cells attempt to reorganize fluxes in order to try to maximize their biomass. However, these reactions are crucial for cancer growth and proliferation and, therefore, the outcome is a deep lowering of the biomass synthesis rate and the fluxes corresponding to the reactions involved in the synthesis of other biomass precursors.

Interruption of glycolysis has produced, as further effect, the annulment of the Warburg effect. Indeed, glycolytic reactions correspond also to the top elements in the list of reactions that, if inhibited, cause a decrease of the two indices, AFR and EOR, connected to the quantification of the Warburg effect. In this context, we observed no production and secretion of lactate and, at the same time, a marked increase of the mitochondrial respiration. Cancer cells must bypass the missed production of ATP through glycolysis (which constitutes the main source for the production of ATP in tumor cells), enhancing the OXPHOS rate. However, clearly, this is not the optimal way for cancer cells to maximize the biomass synthesis and, thus, their growth.

The decrease in tumor biomass production rate caused by the inhibition of glycolytic enzymes supports several features already illustrated in literature. A number of studies focused their attention on the correlation between glycolysis and cancer growth. Indeed, it has been observed that an impaired glycolysis impacts tumor growth in a decisively negative and harmful way, constituting therefore a potential target for the anti-cancer therapy [46]. Many of the glycolytic enzymes and intermediates play a role in several non-glycolytic processes, acting for example in the up-regulation of cell cycle, in the main-

tenance of cellular redox balance, in the chemoresistance and to antagonize the proapoptotic machinery, facilitating in this way cancer cells growth and survival. Moreover, in 2007 Bonnet et al. [52] demonstrated that the reversal of the glycolytic phenotype toward a more active OXPHOS, as we showed in our results, can induce cancer cells death.

In conclusion, in cancer cells an up-regulated glycolysis gives cancer cells an advantage mainly for three reasons: 1) even though this pathway produces a lower quantity of ATP molecules compared to OXPHOS, the rate of ATP production may be 100 times faster with glycolysis [46]; 2) beyond ATP production, an up-regulated glycolysis allows to maintain a high lactate production and secretion, increasing the invasiveness and metastatic potential of the cancer cells; 3) the accumulation of glycolytic enzymes may promote some of the pathways required to increase the tumor mass during growth and proliferation,which are the PPP pathway and the amino acids serine and glycine synthesis.

The inhibition of glycolytic enzymes with specific inhibitors can sharply reduce cancer growth and proliferation. To date, an example of inhibitor (recently entered in the early phase of the clinical trials [46]) is the pyruvate analog 3-bromopyruvate (3-BrPA), which shows a high ability to prevent the tumor glycolysis, as well as a high specificity and selectivity, both in vitro and in vivo, for the glycolytic enzyme glyceraldehyde 3-phosphate dehydrogenase.

4. Conclusions

In this work, we pointed out the potentiality of the mathematical modeling of complex biological systems in relation to the understanding of cancer metabolic rewiring. In order to identify and study the role of all metabolic alterations supporting the neoplastic proliferation, we performed a comparative analysis between a reference and a cancer condition starting from the automatically generated genome-scale networks of the Human Metabolic Atlas database concerning a generic reference cell and three different types of tumor. In the context of cancer cells metabolism, genome-scale modeling represents an increasingly used approach. However, these networks are often not adequately curated and include errors, such as metabolic gaps, that imply the need to perform a further manual curation phase (as occurred in our work). Starting from the chosen genome-scale

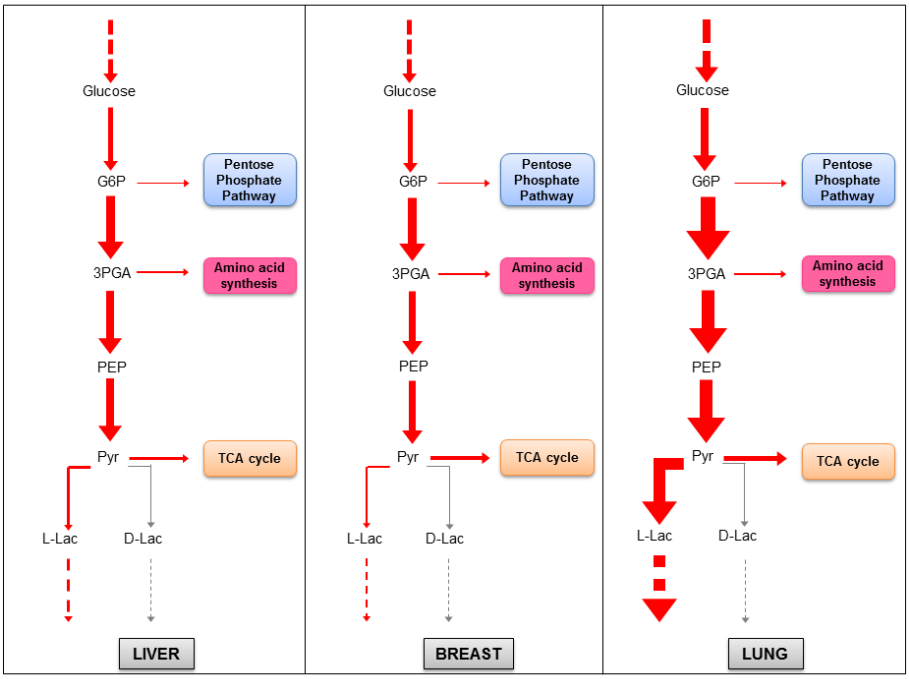

Figure 3: Graphical representation of the metabolic flux redistribution in glycolysis within the three investigated cancer types. An heterogeneous up-regulation of the entire metabolic pathway (indicated by red arrows) emerged in cancer cells with respect to the reference cell. The grey arrows correspond to reactions having a null flux. The thickness of each arrow is proportional to the flux value of the corresponding reaction scaled by 100 for the sake of representation. Abbreviations: G6P, glucose-6-phosphate; 3PGA, 3-phospho-D-glycerate; PEP, phosphoenolpyruvate; Pyr, pyruvate; L-lac, L-lactate; D-lac, D-lactate.

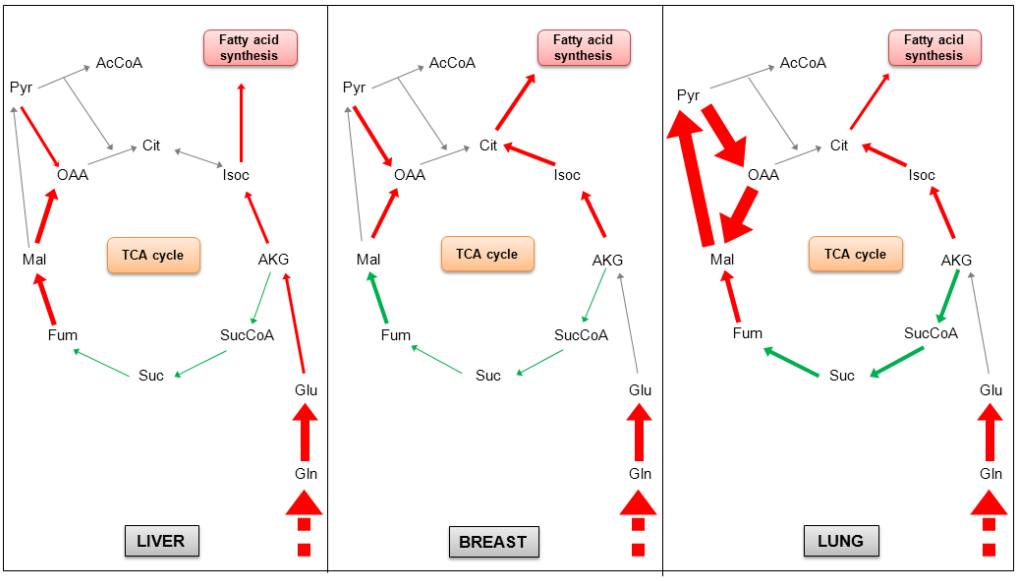

Figure 4: Graphical representation of the metabolic flux redistribution in TCA cycle within the three investigated cancer types. An heterogeneous regulation of the entire metabolic pathway emerged in cancer cells with respect to the reference cell. The red and green arrows correspond, respectively, to the emerged up- and down-regulations. The grey arrows correspond to reactions having a null flux. The thickness of each arrow is proportional to the flux value of the corresponding reaction scaled by 100 for the sake of representation. Abbreviations: Pyr, pyruvate; AcCoA, acetyl-CoA; Cit, citrate; Isoc, isocitrate; AKG, α-ketoglutarate; SucCoA, succinyl-CoA; Suc, succinate; Fum, fumarate; Mal, malate; OAA, oxaloacetate; Gln, glutamine; Glu, glutamate.

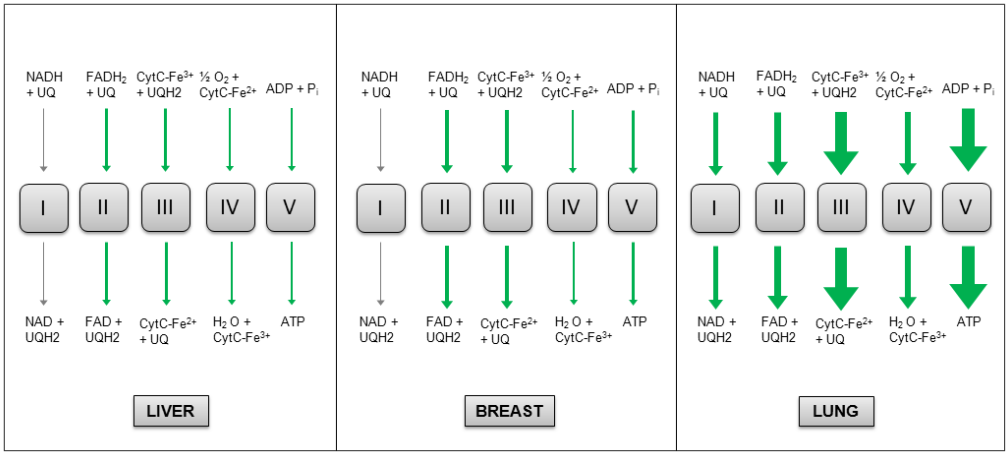

Figure 5: Graphical representation of the metabolic flux redistribution in oxidative phosphorylation within the three investigated cancer types. An heterogeneous down-regulation of the entire metabolic pathway (indicated by green arrows) emerged in cancer cells with respect to the reference cell. The grey arrows correspond to reactions having a null flux. The thickness of each arrow is proportional to the flux value of the corresponding reaction scaled by 100 for the sake of representation. Abbreviations: UQ, ubiquinone; UQH2, ubiquinol; CytC-Fe2+, ferrocytochromeC; CytC-Fe3+, ferricytochromeC.

models, we manually reconstructed core constraint-based metabolic models that zoom-in on cancer metabolic rewiring, considering only specific aspects of metabolism. Unlike genome-scale models, core models are much less difficult to control and their curation may be more accurate.

A constraint-based approach, the Flux Balance Analysis, allowed to identify several metabolic alterations in cancer cells models, which may represent potential targets for the development of therapies able to counteract cancer cells growth and proliferation. Indeed, following the flux distributions analysis in the four core models, we observed a clear distinction between reference and cancer condition under several aspects: growth rate, emergence of the Warburg effect, lactate secretion, glucose and glutamine uptake, TCA cycle, and the oxidative phosphorylation flux values. Two further analyses on the reconstructed core models allowed to detect other potential drug targets, both analyzing the structural differences in core metabolic networks that are responsible for a reversion of the tumoral phenotype towards the reference one, and identifying all the fragility points within the cancer models corresponding to reactions that, if perturbed, cause a negative effect on the system.

The constraint-based models also highlighted a heterogeneity in terms of flux values not only between reference and cancer conditions, but also among the three different cancers, concerning the pathways shown in Figure 3, 4, 5, which are glycolysis, TCA cycle and OXPHOS. This result strengthens the need to focus the attention on several types of tumors rather than on a generic cancer cell, because, although some metabolic features are associated to the three cancers, relevant variations emerged among them. These ones are of great interest in the medical field for the identification of cancer type - specific drug targets in order to develop more effective treatments. The emerged heterogeneity highlights how, given a specific phenotype of interest (cancer, in our case), three different sub-phenotypes may be identified.

On the other hand, the analysis has revealed that some caution is required when dealing with tissue-specific models that have been automatically reconstructed from $-omics$ data. It may indeed happen that, when looking for the optimal "active network", which include the least number of reactions catalyzed by proteins having a low expression level and the greatest number of reactions catalyzed by proteins having a high expression level,

some reactions will be removed from the network, even if they are not necessarily inactive in the corresponding tissue (as it is the case for the reaction 3-phospho-D-glycerate ⇒ 2-phospho-D-glycerate and for inorganic phosphate and water transport reactions mentioned, respectively, in Section 3.1 and 3.3).

In this regard, an approach that is complementary to the reconstruction of distinct tissue-specific networks - and that may represent a possible future development of this work - is the ensemble-evolutionary FBA (eeFBA) approach introduced in [53], which allows to identify ensemble of possible flux distributions of a generic metabolic network that are compatible with different cancer phenotypes.

At last, since we have made the three cancer models comparable among themselves using a common reference model, and in order to identify specific peculiarity linked to a certain type of tissue that is not highlighted using the reference model, a further extension of our work will be the comparison between each of our three cancer core models and their corresponding healthy tissue-specific models recently published within the Human Metabolic Atlas database [54].

Acknowledgement

This work has been supported by the project grant SysBioNet, Italian Roadmap Research Infrastructures 2012. We kindly thank Daniela Besozzi for constructive discussions and criticism and Nataliya Khomchyna for the linguistic revision.

References

[1] J. J. Hornberg, F. J. Bruggeman, H. V. Westerhoff, J. Lankelma, Cancer: a systems biology disease., Biosystems 83 (2-3) (2006) 81–90. doi:10.1016/j.biosystems.2005.05.014.

[2] M. G. Vander Heiden, L. C. Cantley, C. B. Thompson, Understanding the Warburg effect: the metabolic requirements of cell proliferation., Science 324 (5930) (2009) 1029–33. doi:10.1126/science.1160809.

[3] J. W. Locasale, L. C. Cantley, Altered metabolism in cancer., BMC Biol 8 (2010) 88. doi:10.1186/1741-7007-8-88.

[4] C. M. Metallo, P. A. Gameiro, E. L. Bell, K. R. Mattaini, J. Yang, K. Hiller, C. M. Jewell, Z. R. Johnson, D. J. Irvine, L. Guarente, et al., Reductive glutamine metabolism by IDH1 mediates lipogenesis under hypoxia, Nature 481 (7381) (2012) 380–384. doi:10.1038/nature10602.

[5] L. Alberghina, D. Gaglio, Redox control of glutamine utilization in cancer, Cell Death Dis 5 (12) (2014) e1561. doi:10.1038/cddis.2014.513.

[6] L. Alberghina, H. V. Westerhoff, Systems biology: definitions and perspectives, Springer, 2005.

[7] H. Kitano, Perspectives on systems biology, New generation Computing 18 (3) (2000) 199–216. doi:10.1007/BF03037529.

[8] H. Kitano, Systems biology: Toward system-level understanding of biological systems, in: K. H. (Ed.), Foundations of Systems Biology, MIT Press, 2001, pp. 1–36. doi:10.1007/978-1-84882-023-4.

[9] H. Kitano, Systems biology: a brief overview, Science 295 (5560) (2002) 1662–1664. doi:10.1126/science.1069492.

[10] J. Stelling, Mathematical models in microbial systems biology., Curr Opin Microbiol 7 (5) (2004) 513–8. doi:10.1016/j.mib.2004.08.004.

[11] P. Cazzaniga, C. Damiani, D. Besozzi, R. Colombo, M. S. Nobile, D. Gaglio, D. Pescini, S. Molinari, G. Mauri, L. Alberghina, M. Vanoni, Computational strategies for a system-level understanding of metabolism., Metabolites 4 (4) (2014) 1034–87. doi:10.3390/metabo4041034.

[12] N. C. Duarte, S. A. Becker, N. Jamshidi, I. Thiele, M. L. Mo, T. D. Vo, R. Srivas, B. Ø. Palsson, Global reconstruction of the human metabolic network based on genomic and bibliomic data, PNAS 104 (6) (2007) 1777–1782. doi:10.1073/pnas.0610772104.

[13] H. Ma, A. Sorokin, A. Mazein, A. Selkov, E. Selkov, O. Demin, I. Goryanin, The Edinburgh human metabolic network reconstruction and its functional analysis., Mol Syst Biol 3 (2007) 135. doi:10.1038/msb4100177.

[14] T. Hao, H.-W. Ma, X.-M. Zhao, I. Goryanin, Compartmentalization of the Edinburgh human metabolic network., BMC Bioinformatics 11 (2010) 393. doi:10.1186/1471-2105-11-393.

[15] I. Thiele, N. Swainston, R. M. Fleming, A. Hoppe, S. Sahoo, M. K. Aurich, H. Haraldsdottir, M. L. Mo, O. Rolfsson, M. D. Stobbe, et al., A community-driven global reconstruction of human metabolism., Nat Biotechnol 31 (5) (2013) 419–25. doi:10.1038/nbt.2488.

[16] O. Folger, L. Jerby, C. Frezza, E. Gottlieb, E. Ruppin, T. Shlomi, Predicting selective drug targets in cancer through metabolic networks., Mol Syst Biol 7 (2011) 501. doi:10.1038/msb.2011.35.

[17] R. Agren, S. Bordel, A. Mardinoglu, N. Pornputtapong, I. Nookaew, J. Nielsen, Reconstruction of genome-scale active metabolic networks for 69 human cell types and 16 cancer types using INIT., PLoS Comput Biol 8 (5) (2012) e1002518. doi:10.1371/journal.pcbi.1002518.

[18] R. Agren, A. Mardinoglu, A. Asplund, C. Kampf, M. Uhlen, J. Nielsen, Identification of anticancer drugs for hepatocellular carcinoma through personalized genome-scale metabolic modeling, Mol Syst Biol 10 (2014) 721. doi:10.1002/msb.145122.

[19] F. Gatto, I. Nookaew, J. Nielsen, Chromosome 3p loss of heterozygosity is associated with a unique metabolic network in clear cell renal carcinoma., National Acad Sciences 111 (9) (2014) E866–75. doi:10.1073/pnas.1319196111.

[20] J. Ferlay, I. Soerjomataram, M. Ervik, R. Dikshit, S. Eser, C. Mathers, M. Rebelo, D. Forman, F. Bray, GLOBOCAN 2012 v1. 0, Cancer Incidence and Mortality Worldwide: IARC CancerBase

No. 11 [Internet]. Lyon, Fr Int Agency Res Cancer (2013).

[21] F. Bray, J.-S. Ren, E. Masuyer, J. Ferlay, Estimates of global cancer prevalence for 27 sites in the adult population in 2008, International Journal of Cancer 132 (5) (2013) 1133–1145. doi:10.1002/ijc.27711.

[22] J. Hu, J. W. Locasale, J. H. Bielas, J. O'Sullivan, K. Sheahan, L. C. Cantley, M. G. Vander Heiden, D. Vitkup, Heterogeneity of tumor-induced gene expression changes in the human metabolic network, Nature biotechnology 31 (6) (2013) 522–529. doi:10.1038/nbt.2530.

[23] D. A. Fell, J. R. Small, Fat synthesis in adipose tissue. an examination of stoichiometric constraints., Biochem. J 238 (1986) 781–786.

[24] A. Varma, B. Ø. Palsson, Metabolic capabilities of *Escherichia* coli: I. synthesis of biosynthetic precursors and cofactors, Journal of theoretical biology 165 (4) (1993) 477–502.

[25] A. Varma, B. Ø. Palsson, Metabolic capabilities of *Escherichia* coli II. optimal growth patterns, Journal of Theoretical Biology 165 (4) (1993) 503–522.

[26] J. D. Orth, I. Thiele, B. Ø. Palsson, What is flux balance analysis?, Nat Biotechnol 28 (3) (2010) 245–8. doi:10.1038/nbt.1614.

[27] K. Raman, N. Chandra, Flux balance analysis of biological systems: applications and challenges., Brief Bioinform 10 (4) (2009) 435–49. doi:10.1093/bib/bbp011.

[28] P. Romero, J. Wagg, M. L. Green, D. Kaiser, M. Krummenacker, P. D. Karp, Computational prediction of human metabolic pathways from the complete human genome, Genome Biology 6 (1) (2004) R2. doi:10.1186/gb-2004-6-1-r2.

[29] M. Kanehisa, S. Goto, KEGG: kyoto encyclopedia of genes and genomes, Nucleic Acids Res 28 (1) (2000) 27–30. doi:10.1093/nar/28.1.27.

[30] M. Kanehisa, S. Goto, Y. Sato, M. Kawashima, M. Furumichi, M. Tanabe, Data, information, knowledge and principle: back to metabolism in KEGG, Nucleic Acids Res 42 (D1) (2014) D199–D205. doi:10.1093/nar/gkt1076.

[31] M. Uhlén, E. Björling, C. Agaton, C. A.-K. Szigyarto, B. Amini, E. Andersen, A.-C. Andersson, P. Angelidou, A. Asplund, C. Asplund, et al., A human protein atlas for normal and cancer tissues based on antibody proteomics, Molecular & Cellular Proteomics 4 (12) (2005) 1920–1932. doi:10.1074/mcp.M500279-MCP200.

[32] D. S. Wishart, D. Tzur, C. Knox, R. Eisner, A. C. Guo, N. Young, D. Cheng, K. Jewell, D. Arndt, S. Sawhney, et al., HMDB: the human metabolome database, Nucleic acids research 35 (suppl 1) (2007) D521–D526. doi:10.1093/nar/gkl923.

[33] D. S. Wishart, C. Knox, A. C. Guo, R. Eisner, N. Young, B. Gautam, D. D. Hau, N. Psychogios, E. Dong, S. Bouatra, et al., HMDB: a knowledgebase for the human metabolome, Nucleic acids research 37 (suppl 1) (2009) D603–D610. doi:10.1093/nar/gkn810.

[34] D. S. Wishart, T. Jewison, A. C. Guo, M. Wilson, C. Knox, Y. Liu, Y. Djoumbou, R. Mandal, F. Aziat, E. Dong, et al., HMDB 3.0 the human metabolome database in 2013, Nucleic acids research (2012) gks1065doi:10.1093/nar/gks1065.

[35] O. Resendis-Antonio, A. Checa, S. Encarnacin, Modeling core metabolism in cancer cells: Surveying

the topology underlying the Warburg effect, PLoS ONE 5 (8) (2010) e12383. doi:10.1371/journal.pone.0012383.

[36] P. Shannon, A. Markiel, O. Ozier, N. S. Baliga, J. T. Wang, D. Ramage, N. Amin, B. Schwikowski, T. Ideker, Cytoscape: a software environment for integrated models of biomolecular interaction networks., Genome Res 13 (11) (2003) 2498–504. doi:10.1101/gr.1239303.

[37] M. S. Cline, M. Smoot, E. Cerami, A. Kuchinsky, N. Landys, C. Workman, R. Christmas, I. Avila-Campilo, M. Creech, B. Gross, et al., Integration of biological networks and gene expression data using Cytoscape., Nat Protoc 2 (10) (2007) 2366–82. doi:10.1038/nprot.2007.324.

[38] A.-L. Barabsi, Z. N. Oltvai, Network biology: understanding the cell's functional organization., Nat Rev Genet 5 (2) (2004) 101–13. doi:10.1038/nrg1272.

[39] S. A. Becker, A. M. Feist, M. L. Mo, G. Hannum, B. Ø. Palsson, M. J. Herrgard, Quantitative prediction of cellular metabolism with constraint-based models: the COBRA toolbox., Nat Protoc 2 (3) (2007) 727–38. doi:10.1038/nprot.2007.99.

[40] J. Schellenberger, R. Que, R. M. T. Fleming, I. Thiele, J. D. Orth, A. M. Feist, D. C. Zielinski, A. Bordbar, N. E. Lewis, S. Rahmanian, et al., Quantitative prediction of cellular metabolism with constraint-based models: the COBRA toolbox v2.0., Nat Protoc 6 (9) (2011) 1290–307. doi:10.1038/nprot.2011.308.

[41] D. De Martino, F. Capuani, M. Mori, A. De Martino, E. Marinari, Counting and correcting thermodynamically infeasible flux cycles in genome-scale metabolic networks, Metabolites 3 (4) (2013) 946–966. doi:10.3390/metabo3040946.

[42] K. Yizhak, S. E. Le Dvdec, V. M. Rogkoti, F. Baenke, V. C. de Boer, C. Frezza, A. Schulze, B. van de Water, E. Ruppin, A computational study of the Warburg effect identifies metabolic targets inhibiting cancer migration., Mol Syst Biol 10 (2014) 744. doi:10.15252/msb.20134993.

[43] C. Li, M. Donizelli, N. Rodriguez, H. Dharuri, L. Endler, V. Chelliah, L. Li, E. He, A. Henry, M. I. Stefan, et al., BioModels Database: An enhanced, curated and annotated resource for published quantitative kinetic models, BMC systems biology 4 (1) (2010) 92. doi:10.1186/1752-0509-4-92.

[44] R. J. DeBerardinis, A. Mancuso, E. Daikhin, I. Nissim, M. Yudkoff, S. Wehrli, C. B. Thompson, Beyond aerobic glycolysis: transformed cells can engage in glutamine metabolism that exceeds the requirement for protein and nucleotide synthesis., Proc Natl Acad Sci U S A 104 (49) (2007) 19345–50. doi:10.1073/pnas.0709747104.

[45] D. Hanahan, R. A. Weinberg, Hallmarks of cancer: the next generation., Cell 144 (5) (2011) 646–74. doi:10.1016/j.cell.2011.02.013.

[46] S. Ganapathy-Kanniappan, J.-F. H. Geschwind, Tumor glycolysis as a target for cancer therapy: progress and prospects., Mol Cancer 12 (2013) 152. doi:10.1186/1476-4598-12-152.

[47] R. J. DeBerardinis, J. J. Lum, G. Hatzivassiliou, C. B. Thompson, The biology of cancer: metabolic reprogramming fuels cell growth and proliferation., Cell Metab 7 (1) (2008) 11–20. doi:10.1016/j.cmet.2007.10.002.

[48] K. Hiller, C. M. Metallo, Profiling metabolic networks to study cancer metabolism., Curr Opin Biotechnol 24 (1) (2013) 60–8. doi:10.1016/j.copbio.2012.11.001.

[49] H. Z. Mullen A.R., Oxidation of alpha-ketoglutarate is required for reductive carboxylation in cancer cells with mitochondrial defects, Cell reports 7 (5) (2014) 1679–1690. doi:10.1016/j.celrep.2014.04.037.

[50] R. J. DeBerardinis, T. Cheng, Q's next: the diverse functions of glutamine in metabolism, cell biology and cancer, Oncogene 29 (3) (2010) 313–324. doi:10.1038/onc.2009.358.

[51] J. Hooda, D. Cadinu, M. M. Alam, A. Shah, T. M. Cao, L. A. Sullivan, R. Brekken, L. Zhang, Enhanced heme function and mitochondrial respiration promote the progression of lung cancer cells., PLoS One 8 (5) (2013) e63402. doi:10.1371/journal.pone.0063402.

[52] S. Bonnet, S. L. Archer, J. Allalunis-Turner, A. Haromy, C. Beaulieu, R. Thompson, C. T. Lee, G. D. Lopaschuk, L. Puttagunta, S. Bonnet, et al., A mitochondria-K^+ channel axis is suppressed in cancer and its normalization promotes apoptosis and inhibits cancer growth., Cancer cell 11 (1) (2007) 37–51. doi:10.1016/j.ccr.2006.10.020.

[53] C. Damiani, D. Pescini, R. Colombo, S. Molinari, L. Alberghina, M. Vanoni, G. Mauri, An ensemble evolutionary constraint-based approach to understand the emergence of metabolic phenotypes, Natural Computing 13 (3) (2014) 321–331. doi:10.1007/s11047-014-9439-4.

[54] M. Uhlén, L. Fagerberg, B. M. Hallström, C. Lindskog, P. Oksvold, A. Mardinoglu, Å. Sivertsson, C. Kampf, E. Sjöstedt, A. Asplund, et al., Tissue-based map of the human proteome, Science 347 (6220) (2015) 1260419. doi:10.1126/science.1260419.

Potential Reviewers

We confirm the list of potential reviewers provided during the first submission.

List of Potential Reviewers:

1. **Daniele De Martino**
   Center for life nanoscience, Istituto Italiano di Tecnologia, CLNS-IIT
   Viale Regina Elena 291, 00161, Rome, Italy
   daniele.demartino@roma1.infn.it

2. **Osbaldo Resendis-Antonio**
   Laboratory of Human Systems Biology, Instituto Nacional de Medicina Genómica (INMEGEN), México, DF, Mexico
   oresendis@inmegen.gob.mx